

# A novel design of a compact multilayer resonator using double-sided microstrip

M. M. POTREBIĆ\*, D. V. TOŠIĆ

*School of Electrical Engineering, University of Belgrade, P.O. Box 35-54, 11120 Belgrade, Serbia*

A novel design of a compact multilayer resonator is proposed using a double-sided microstrip. This resonator consists of two quasi-lumped elements: a square spiral inductor and a microstrip patch capacitor. Each quasi-lumped element is printed on different layers – the upper and the lower dielectric layer separated by a common ground plane. The maximum dimension of this resonator is less than  $\lambda_g/25$ , where  $\lambda_g$  is the guided wavelength of a  $50\ \Omega$  microstrip line at the resonant frequency. The design methodology is exemplified by a second-order multilayer bandpass filter that is based on the proposed resonator. The filter is fabricated and measured, and the simulated and measured results are in agreement.

(Received January 25, 2012; accepted April 11, 2012)

*Keywords:* Double-sided microstrip, Multilayer bandpass filter, Quasi-lumped resonator

## 1. Introduction

With the development of modern wireless communications, designing compact and high-performance microwave filters in communication systems is largely required.

In general, microstrip resonators for the filter design may be classified as lumped-element or quasi-lumped-element resonators and distributed line or patch resonators [1, ch. 4]. Typical distributed line resonators are the half-wavelength and the quarter-wavelength resonators, while the sizes of lumped-element resonators are much smaller than the operating wavelength. Although lumped-element resonators typically exhibit a lower quality factor than distributed line resonators due to smaller dimensions, they have the advantage of smaller size, lower cost, and wider bandwidth characteristics [2].

Since the small size requirements are often of prime importance for filter design, to reduce the size of filter realizations, we have proposed a novel multilayer resonator which is implemented on a double-sided microstrip. The resonator consists of two quasi-lumped elements: an inductor and a capacitor, where each of them is printed on outer sides of two dielectric substrates with a common ground in between. A square spiral inductor and a microstrip patch (serving as a capacitor) are connected by a via hole which passes through the structure without electrical connection to the common ground plane. With this approach, the arrangement of components is no longer limited to a single plane and, thus, the design becomes flexible [3].

In this study, based on the proposed resonator, a second-order coupled-resonator bandpass filter is designed. We explain the design methodology and show the results generated by electromagnetic (EM) simulation. In addition, we present the measurement results made on the fabricated structure. Hence, conclusions are drawn about the

performance of the analyzed structure: frequency response and footprint.

## 2. Compact multilayer resonators in double-sided microstrip configuration

The newly proposed resonator is mainly composed of three elements, i.e., the square spiral inductor on the top plane, the connecting via through the substrate, and the microstrip patch on the bottom plane. Fig. 1 shows the three-dimensional electromagnetic (3D EM) model of the proposed multilayer resonator (spiral-via-patch resonator). The cross section of the resonator with a common ground plane is depicted in Fig. 2.

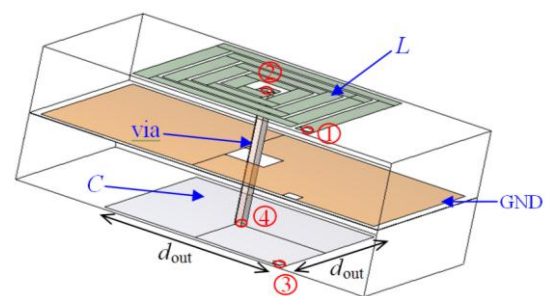


*Fig. 1. 3D EM model of the multilayer resonator.*

If the microstrip patch has a square shape with the area  $d_{out} \times d_{out}$ , we fix the footprint of the spiral inductor to the same area  $d_{out} \times d_{out}$ . The inductor and the capacitor of this resonator have the same occupied planar size. The patch on the bottom-plane is located exactly beneath the spiral on

the top plane, which is important for easy arrangement of coupled-resonator pairs to simultaneously provide electrical and magnetic couplings. There are two ways to connect the inductor and the capacitor, Fig. 1. First, the innermost turn of the inductor (node 2) is connected to the center of the capacitor patch (node 4) – “center connection”. Secondly, the outermost turn of the inductor (node 1) is connected to the corner of the capacitor patch (node 3) – “corner connection”.

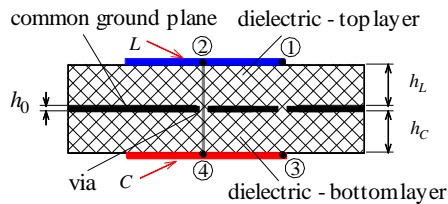


Fig. 2. The cross section of the multilayer resonator.

The approximate lumped-element equivalent circuit of the proposed resonator is presented in Fig. 3. Approximate expressions for the inductance ( $L$ ), parasitic capacitances to ground ( $C_{11}$  and  $C_{12}$ ), and resistance ( $R_L$ ) for a square spiral inductor calculated as in [2, p. 27, eq. 2.18]. The inductance  $L_{\text{via}}$ , and the resistance  $R_{\text{via}}$  of a cylindrical via hole may be approximately calculated as in [2, p. 283, eq. 9.1]. The length of the connecting via (through via) that passes through the structure, without electrical contact with the common ground plane, is  $H = h_L + h_C + h_0$ .

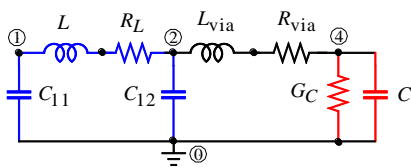


Fig. 3. Circuit model for the resonator of Fig. 1.

Since the capacitance of the microstrip patch deviates from the capacitance of a parallel plate capacitor, we have extracted the corresponding element value using the full-wave electromagnetic simulator at the resonant frequency [4].

The dimensions of major resonator parameters, such as the patch area, spiral line width, and spiral line length, to provide a given response, are basically affected by the substrate. To be specific, hereafter, all circuits in this study will be realized on an RT/duroid 5880 board ( $\epsilon_r = 2.2$ ,  $h = 1.575$  mm,  $\tan \delta = 0.001$ ,  $t = 18$   $\mu\text{m}$ ), that is  $h_C = h_L = h$  and  $h_0 = 2t$ .

The spiral-via-patch resonator is designed and adjusted to provide the resonant frequency at 1.7 GHz. The parameters of the square spiral inductor are  $N$  (number of

turns),  $w$  (spiral line width),  $s$  (turn spacing), and  $d_{\text{out}}$  (effective outer dimension) or  $d_{\text{in}}$  (effective inner dimension), Fig. 4. Dimensions are given in Table 1. The capacitor patch has a square shape with the area  $d_{\text{out}} \times d_{\text{out}}$ . The extracted lumped-element values are given in Table 2.

Table 1. Dimensions of the square spiral inductor.

$N$	$w$ [mm]	$s$ [mm]	$d_{\text{out}}$ [mm]	$d_{\text{in}}$ [mm]
4	0.4	0.1	4.6	0.8

With the favor of a double-sided microstrip configuration, the novel spiral-via-patch resonator is compact and has a size of only  $4.6\text{mm} \times 4.6\text{mm}$  (i.e.,  $0.036\lambda_g \times 0.036\lambda_g$ ) which is smaller more than 30% compared to the two-layer structure [5] and the dual-metal plane configuration (CPW realization) [3].

Table 2. Extracted lumped-element values of Fig. 3.

$L$ [nH]	$R_L$ [ $\Omega$ ]	$C_{11}$ [pF]	$C_{12}$ [pF]	$C$ [pF]	$G_C$ [ $\mu\text{S}$ ]	$L_{\text{via}}$ [nH]	$R_{\text{via}}$ [ $\Omega$ ]
33.87	1.59	0.34	0.25	0.61	0.11	1.86	0.25

Using the extraction technique provided in [6] the unloaded quality factor  $Q_u$  associated with the proposed resonator is found about 130, which is more than two times compared to realizations reported in [3], [5].

To increase the capacitance value per unit area of the resonator we propose two realizations of the capacitor. First, it is decreased the substrate thickness on the bottom layer of the structure, i.e. dielectric layer sandwich between two electrodes is decreased. With this procedure the capacitance value may be increased around six times with decrease of the thickness of dielectric layer around 12.4 times, Fig. 5. Alternatively, a multilayer capacitor can be used, Fig. 6. This capacitor is commonly known as a multilayer capacitor having  $n$  plates. The capacitance value of a multilayer capacitor (with  $n$  plates) is directly proportional to the number of plates ( $C \sim n - 1$ ).

To characterize the proposed resonator, the fundamental resonant frequency is simulated, using different realizations of the capacitor: (a) different thickness of dielectric layer sandwich between two electrodes (Fig. 2) and (b) multilayer capacitor with 3 plates (Fig. 6). The simulation results are given in Table 3. (Note that  $-40 < S_{21}[\text{dB}] < -30$ , see [6].)

### 3. Equivalent lumped-element circuits for compact multilayer resonators

The equivalent circuit, that is required to design the proposed resonator and to determine the resonant

frequencies, will be derived here. Fig. 7 shows the approximate lumped-element equivalent-circuit model for the proposed resonator with (a) “center connection”, (b) “corner connection”, (c) “corner connection” and grounded inductor (the outermost turn of the inductor is connected to the common ground plane by a via modeled with  $L_{\text{viaGND}}$  and  $R_{\text{viaGND}}$ ). The input admittances (for the three cases) may be formulated as

$$Y_{\text{in1}} = sC_{11} + \frac{1}{sL + R_L + \frac{1}{sC_{12} + \frac{1}{sL_{\text{via}} + R_{\text{via}} + \frac{1}{sC + G_C}}}}, \quad (1)$$

$$Y_{\text{in2}} = sC_{11} + 1/sL_{\text{via}} + R_{\text{via}} + (sC + G_C)^{-1} + 1/(sL + R_L + (sC_{12})^{-1}) \quad (2)$$

$$Y_{\text{in3}} = sC_{11} + 1/(sL_{\text{via}} + R_{\text{via}} + (sC + G_C)^{-1}) + 1/(sL + R_L + (sC_{12} + 1/(R_{\text{viaGND}} + sL_{\text{viaGND}}))^{-1}). \quad (3)$$

Using the approximation:  $L_{\text{via}} \rightarrow 0$ ,  $R_{\text{via}} \rightarrow 0$ ,  $R_L \rightarrow 0$ ,  $G_C \rightarrow 0$ ,  $C_{11} = C_{12}$ ,  $L_{\text{viaGND}} \rightarrow 0$ ,  $R_{\text{viaGND}} \rightarrow 0$ , the input admittances are given by

$$Y_{\text{in1}} \approx sC_{11} + 1/(sL + 1/(s(C + C_{11}))^{-1}), \quad (4)$$

$$Y_{\text{in2}} \approx s(C + C_{11}) + 1/(sL + (sC_{11})^{-1}), \quad (5)$$

$$Y_{\text{in3}} \approx s(C + C_{11}) + 1/sL. \quad (6)$$

The parallel resonant frequencies occur as  $Y_{\text{in}i} = 0$  ( $i = 1, 2, 3$ ), which yields the angular frequencies

$$\omega_{r1} = \sqrt{(C + 2C_{11})/(LC_{11}(C + C_{11}))}, \quad \omega_{r2} = \omega_{r1}, \quad (7)$$

$$\omega_{r3} = 1/\sqrt{L(C + C_{11})}. \quad (8)$$

The resonator realizations with “center connection” and “corner connection” have the same resonant frequency. If the parasitic capacitances to ground  $C_{11}$  and  $C_{12}$  are negligible, i.e.  $C_{11}, C_{12} \ll C$  than  $\omega_{r1} = \omega_{r2} \approx 1/\sqrt{LC_{11}}$  and  $\omega_{r3} \approx 1/\sqrt{LC}$ .

With respect to the three different realizations of a single spiral-via-patch resonator (Fig. 7), the corresponding resonant frequencies are given in Table 4. The dimensions of the resonator are given in Table 1, and the corresponding lumped-element values are in Table 2,  $L_{\text{viaGND}} = 0.996 \text{ nH}$  and  $R_{\text{viaGND}} = 0.13 \Omega$ .

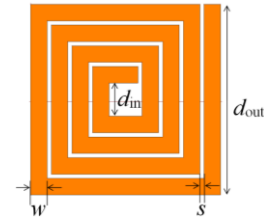


Fig. 4. The configuration of a square spiral inductor.

#### 4. Implementation of a second-order filter and experimental results

To demonstrate the feasibility of realizing a filter with the proposed resonator (shown in Fig. 1), a second-order filter is designed with the center frequency  $f_0$  at 1.7 GHz and 3dB fractional bandwidth of 4% (Fig. 8). The coupling coefficient between the two resonators is  $K_{12} = 0.028$  and the external quality factors, associated with the resonators and the feeding lines, are  $Q_{ei} = Q_{eo} = 50$ . To satisfy this specification, the coupling gap  $s_{12}$  is chosen as 2mm and  $s_0$  as 0.1mm.

The initial filter dimensions are in Table 1. To meet the specification, these dimensions are optimized similarly as in [7]. The filter ports increase the resonator capacitance, decrease the resonant frequency, so we reduced the length of the spiral inductor for about 1.125 turns.

The top- and bottom-plane of the fabricated filter are shown in Fig. 9. The filter is measured using the Agilent E5062A network analyzer.

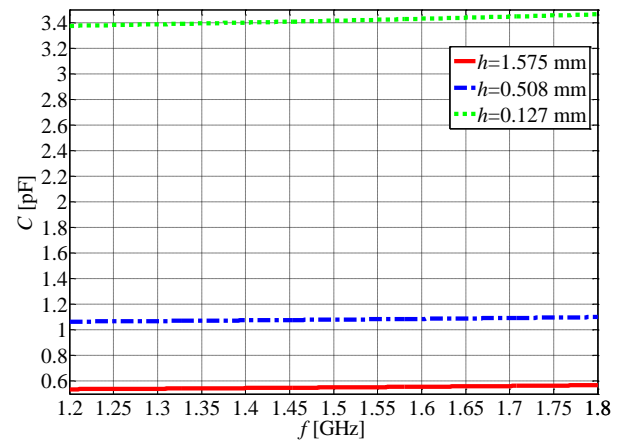


Fig. 5. Patch capacitance for different thickness ( $h$ ).

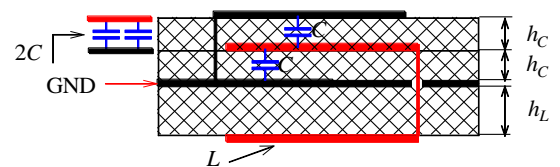


Fig. 6. Multiplate capacitor with  $n = 3$  plates.

Table 3. Resonant frequencies with respect to different realizations of the capacitor presented in Figs. 2, 6.

	Resonator in Fig. 2			Resonator in Fig 6
$h_C$ [mm]	1.575	0.508	0.127	0.127
$S_{21}$ [dB]	-32.49	-32.31	-31.26	-30.87
$f_0$ [GHz]	1.698	1.629	1.496	1.461

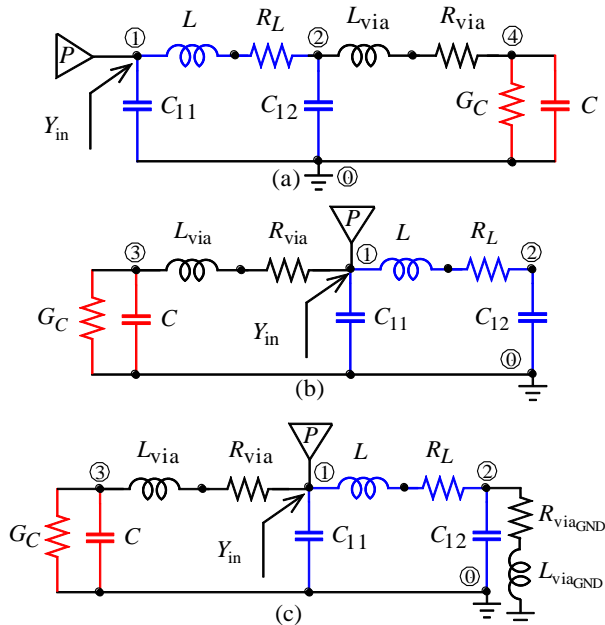


Fig. 7. Equivalent circuits for the resonator (from Fig. 1) with (a) "center connection", (b) "corner connection", (c) "corner connection" and grounded inductor.

The simulated and measured response of the fabricated filter is shown in Fig. 10a. Measured results have validated the theoretical analysis well. The filter has an insertion loss of 2.45 dB at the central frequency (1.708 GHz) due to the conductor and dielectric losses. The conductor losses dominate. The measured 3dB fractional bandwidth is approximately 4%. The first spurious passband ( $f_{spl}$ ) occurs at 7.395 GHz ( $4.33 f_0$ ), Fig. 10b.

The fabricated filter possesses a compact size of  $11.2\text{mm} \times 4.6\text{mm}$  (i.e.,  $0.087\lambda_g \times 0.036\lambda_g$ ), which is much smaller compared to the conventional single layer filter [1, ch. 5] and more than 30% smaller than two-layer realization reported in [5]. The miniaturized size of this filter reveals the advantage of using the proposed spiral-via-patch resonators for filter design.

Table 4. Resonant frequencies of the resonator for three different realizations (Fig. 7).

REALIZATIONS	$f_r$ [GHz]	
	CIRCUIT, Fig. 7	3D EM simulation
center connection	1.724	1.719
corner connection	1.928	1.903
grounded inductor	0.862	0.814

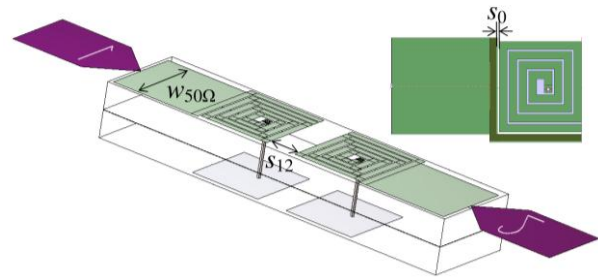


Fig. 8. 3D EM model of the multilayer filter.

## 5. Conclusions

We have studied realizations of a compact multilayer resonator which is implemented on a double-sided microstrip. A novel resonator has been proposed and it consists of two quasi-lumped elements, a square spiral inductor and a microstrip patch capacitor. The quasi-lumped elements are printed on different layers separated by a common ground plane.

The benefit of the proposed multilayer resonator is its compact design and a reduction of the footprint to  $0.036\lambda_g \times 0.036\lambda_g$ .

Design methodology has been presented and validated by EM simulation. The multilayer filter has been fabricated, measured, and the experimental results are in good agreement with the theoretical and simulation results.

## Acknowledgments

The authors would like to thank the Serbian Ministry of Education and Science for financial support under project TR32005.

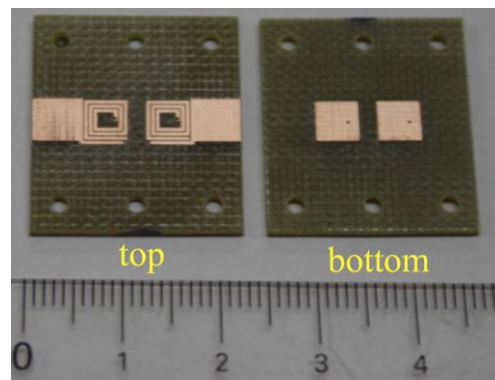
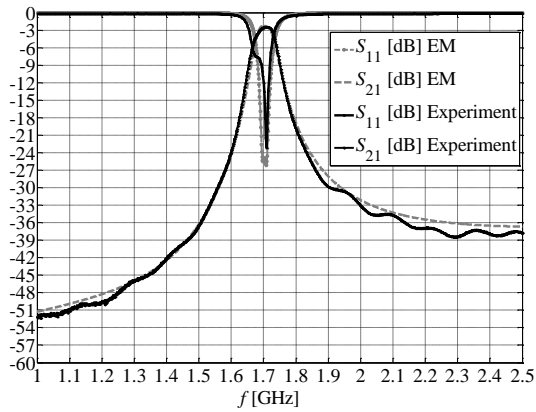
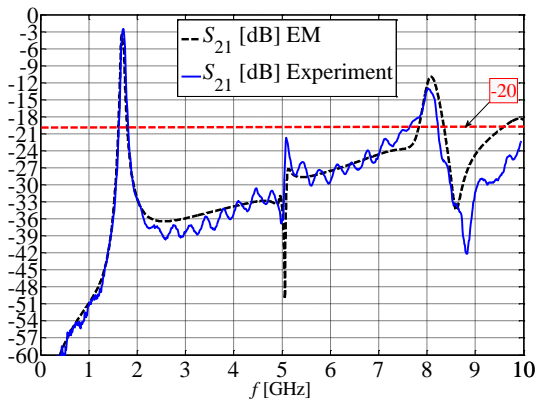


Fig. 9. Photograph of the fabricated filter.



(a)



(b)

Fig. 10.  $S$ -parameters of the proposed filter: EM simulation and experiment: (a) zoom, (b) full band.

## References

- [1] J.-S. Hong, *Microstrip Filters for RF/Microwave Applications*, Wiley, New York (2011).
- [2] I. J. Bahl, *Lumped Elements for RF and Microwave Circuits*, Artech House, Norwood, MA (2003).
- [3] S.-C. Lin, C.-H. Wang, C. H. Chen, *IEEE Trans. Microw. Theory Tech.* **55**, 137 (2007).
- [4] *IE3D-Full-Wave EM Simulation, Optimization, and Synthesis Package*, Zeland Software, Inc., Fremont, CA (2007).
- [5] C.-H. Chen, C.-H. Huang, T.-S. Horng, S.-M. Wu, J.-Y. Li, C.-C. Chen, C.-T. Chiu, C.-P. Hung, *IEEE Microw. Wireless Compon. Lett.* **19**, 293 (2009).
- [6] D. G. Swanson, Jr., *IEEE Microw. Magazine*, **8**, 105, (2007).
- [7] N. Militaru, G. Lojewski, M. G. Banciu, J. Optoelectron. Adv. Mater. **12**, 909 (2010).

\*Corresponding author: milka\_potrebic@etf.rs